The Inverse Kinematics

describes the mapping from the generalized coordinates describing the position and orientation of the moving platform to the joint coordinates.

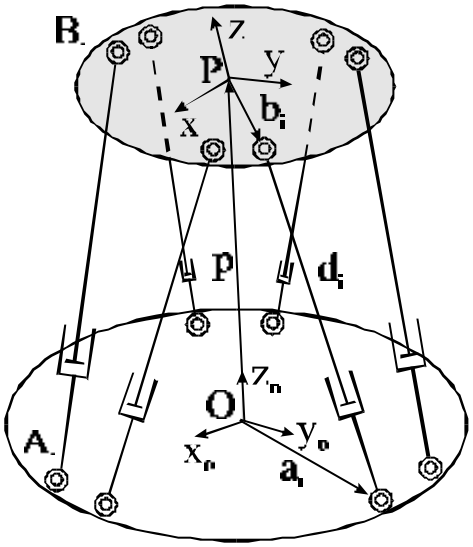

Figure 15. Parameters for the Inverse Kinematic problem.

the Inverse Kinematics problem can be solved by using

$$A_i B_i = \mathbf{p} + R\mathbf{b}_i - \mathbf{a}_i \qquad (1)$$

to extract the joint variables from leg lengths. The length of the i-th leg can be obtained by taking the dot product of the vector A_iB_i with itself, for i:1,…,6 in the form.

$$\mathbf{d}_i^2 = \left[\mathbf{p} + R\mathbf{b}_i - \mathbf{a}_i\right]^T \left[\mathbf{p} + R\mathbf{b}_i - \mathbf{a}_i\right] \qquad (2)$$

The Direct Kinematics problem

describes the mapping from the joint coordinates to the generalized coordinates.

The problem is quite difficult since it involves the solution of a system of non-linear coupled algebraic equations (1), and has many solutions that refer to assembly modes.

$$A_i B_i = \mathbf{p} + R\mathbf{b}_i - \mathbf{a}_i \qquad (1)$$

- For the general case with planar base and platform the Direct Kinematics problem may have up to 40 solutions.
- A 20-th degree polynomial can be derived whose solutions lead to 40 mutually symmetric assembly modes.

Many algorithms

have been proposed for workspace analysis of parallel manipulators but they are usually very cumbersome and numerically not efficient for repetitive computations in design algorithms.

- The position workspace can be defined as the region in the Cartesian space that can be reached by a reference point on the moving platform with a constant orientation.
- On the other hand, orientation workspace is defined as the set of all attainable orientations of the mobile platform about a fixed point and it can be represented in Cartesian, Spherical, or Cylindrical frames.

Orientation workspace is probably the most difficult characteristic of a manipulator to determine and represent.

A general numerical evaluation of the workspace by formulating a suitable binary representation of a cross-section.

- $$i = \left[\frac{x + \Delta x}{x} \right]; \qquad j = \left[\frac{y + \Delta y}{y} \right] \qquad (3)$$

$$P_{ij} = \begin{cases} 0 \text{ if } P_{ij} \notin \mathrm{W(H)} \\ 1 \text{ if } P_{ij} \in \mathrm{W(H)} \end{cases} \qquad (4)$$

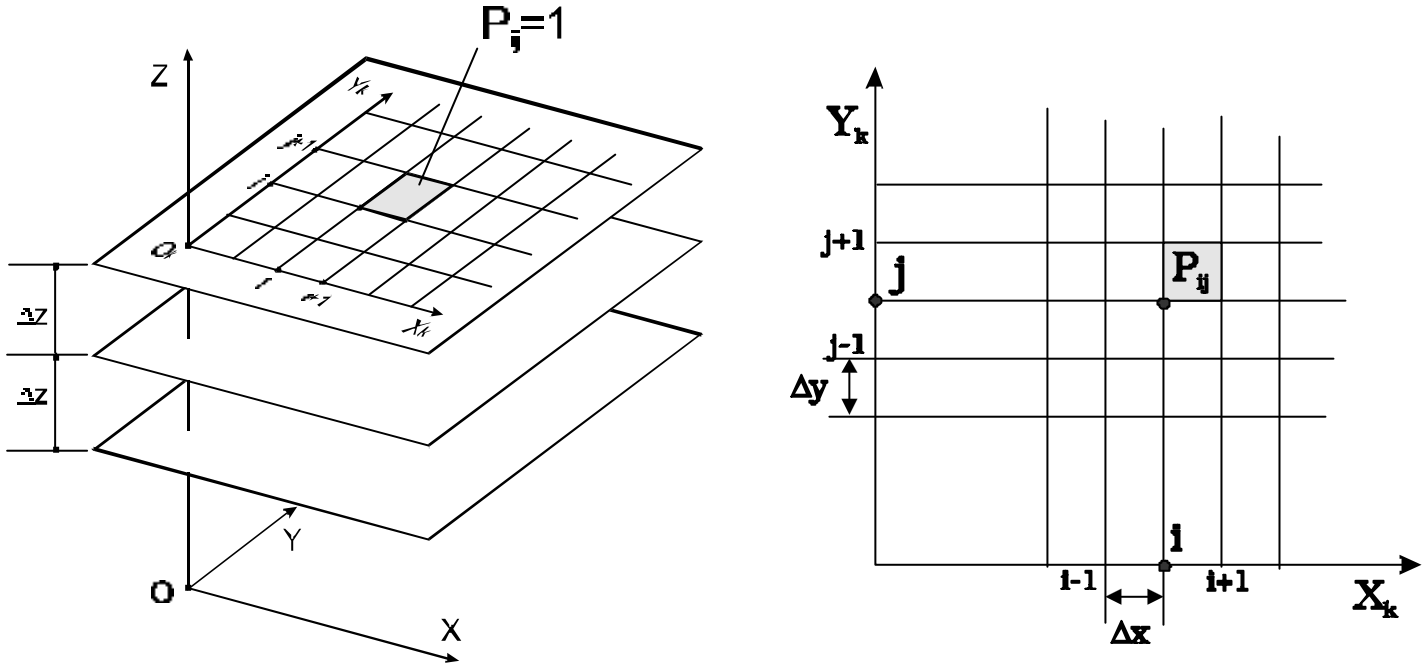

Figure 16 A scheme for binary representation and evaluation of manipulator workspace.

$$A_z = \sum_{i=1}^{i_{max}} \sum_{j=1}^{j_{max}} \left(P_{ij} \, \Delta x \, \Delta y \right) \qquad (5)$$

$$V = \sum_{z=z_{min}}^{z=z_{max}} A_z \, \Delta z \qquad (6)$$

The stiffness properties of a parallel manipulator can be defined through a 6x6 matrix that is called as stiffness matrix K.

$$\mathbf{W} = K \ \Delta \mathbf{S} \tag{7}$$

$$K_{CaPaMan} = M_{FN} \ K_P \ C_P^{-1} \ A_d^{-1}$$

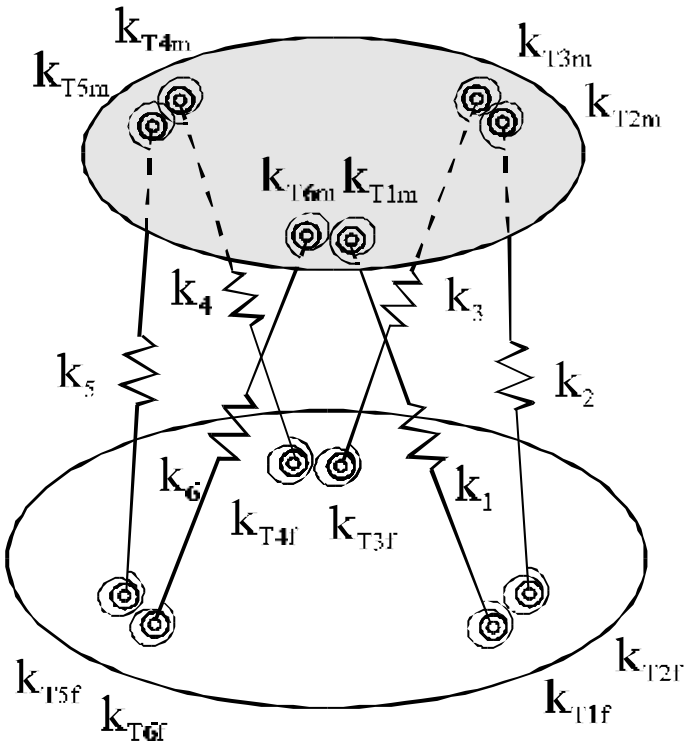

Figure 17. A model for stiffness analysis of parallel manipulators.

One of the most practical drawbacks of parallel manipulators can be considered
the overall size of the mechanical design that occupies considerable volume without any possibility to use it for other equipment.

.

The large payload can be computed by examining the parallel manipulator as a reticular structure and considering the stiffness properties to ensure a desired positioning accuracy.

Similarly, high velocity and high acceleration can be achieved during the operation of parallel manipulators because of their reticular architecture.

- Computation of these characteristics attains to kinematic analysis and simulation of parallel manipulators.

Link interference problem could be solved through an algorithm that allows to check for the workspace in interference-free regions and then to determine in which region the initial assembly modes can be located to obtain the interference-free workspace of the robot. This workspace analysis represents a difficult task even for robots with very simple kinematic chains.

singularity conditions

The instantaneous relationship between the velocity in the Cartesian space and active joint velocity

$$\mathbf{A}\dot{\mathbf{J}} = \mathbf{B}\mathbf{t} \qquad (8)$$

- This expression can be used for a suitable numerical analysis of singularities that can be useful also in experimental tests.

Usually condition of singular configurations can be represented by surfaces in the configuration space and *they can be obtained by vanishing the determinant of the two Jacobian matrices **A** and **B**.*

- In particular, matrix **A** gives the Inverse Kinematics singularities; and **B** gives the Direct Kinematics singularities.

Last ones are inside the workspace and in such configurations a manipulator loses its rigidity becoming locally movable, even if the actuate joints are locked.

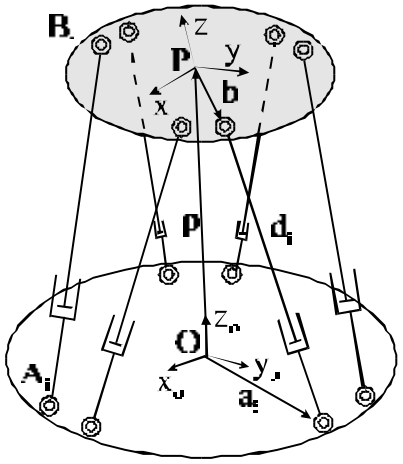

$$\mathbf{B} = \begin{bmatrix} \mathbf{d}_1 & (\mathrm{R}\mathbf{b}_1)\times\mathbf{d}_1 \\ \dots & \dots \\ \mathbf{d}_6 & (\mathrm{R}\mathbf{b}_6)\times\mathbf{d}_6 \end{bmatrix} \qquad (9)$$

4. DESIGN PROBLEMS AND FORMULATION

- The above-mentioned considerations make the design of parallel manipulator a complex task.
- Several different approaches and algorithms have been presented in the literature
- The strong influence of fundamental characteristics to each other will require to consider those formulations in one design model and nowadays this can be achieved with numerical efficiency by using Optimization Techniques.

the optimum design of parallel manipulators a multi-objective optimization problem can be formulated as

$$\min \mathbf{f}(\mathbf{X}) = \left[f_W(\mathbf{X}), f_S(\mathbf{X}), f_K(\mathbf{X}) \right] \quad (10)$$

Subjected to

$$\mathbf{g}(\mathbf{X}) < \mathbf{0} \quad (11)$$

$$\mathbf{h}(\mathbf{X}) = \mathbf{0}$$

- There are a number of alternative methods to solve numerically a multi-objective optimization problem with Eqs. (10) and (11).
- by using a single objective function F(**X**) and standard constrained optimization methods when the number N of objective components is limited.

$$\min F(\mathbf{X}) = \sum_{\mathbf{i}=1}^{\mathbf{N}} w_i f_i(\mathbf{X}) \quad (12)$$

- w_i are weighting factors, which may correspond or be chosen referring to the relative importance of the objectives.
- the objective functions can be formulated as

$$f_1(X) = \left| 1 - \frac{V_{pos}}{V_{posg}} \right| \qquad f_2(X) = \left| 1 - \frac{V_{or}}{V_{org}} \right|$$

$$f_3(X) = \left(1 - \frac{|\Delta x|}{|\Delta x_g|} \right) + \left(1 - \frac{|\Delta y|}{|\Delta y_g|} \right) + \left(1 - \frac{|\Delta z|}{|\Delta z_g|} \right) \quad (13)$$

$$f_4(X) = \left(1 - \frac{|\Delta \varphi|}{|\Delta \varphi_g|} \right) + \left(1 - \frac{|\Delta \psi|}{|\Delta \psi_g|} \right) + \left(1 - \frac{|\Delta \theta|}{|\Delta \theta_g|} \right)$$

$$f_5(X) = \min\left(-\det \mathbf{B}_{nor} \right)$$

The numerical solution of the design problem with Eqs.(12) and (13) can be very cumbersome and even complex when also constraints are considered for assembling operations.

At LARM research activity is carried out and is undergoing to enhance the proposed optimum design formulation for parallel

manipulators by using multi-objective optimization and mechanical interpretation of design criteria.
Satisfactory results have been obtained by looking at suitable interpretation of design criteria and analysis formulations, also for experimental tests of validations.

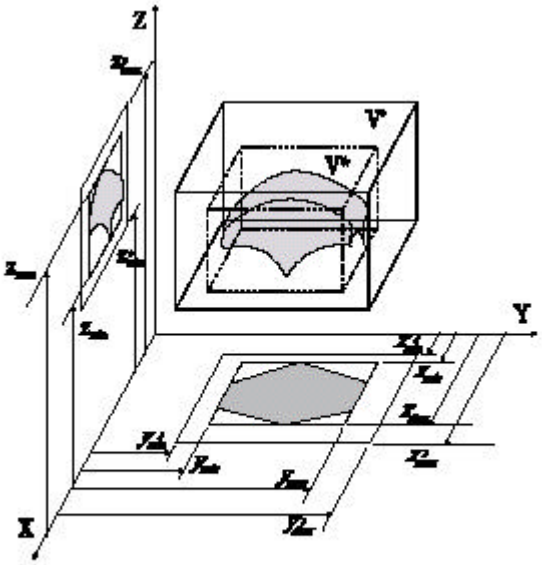

Fig. 1. A numerical approximation for the position workspace volume of CaPaMan manipulator.

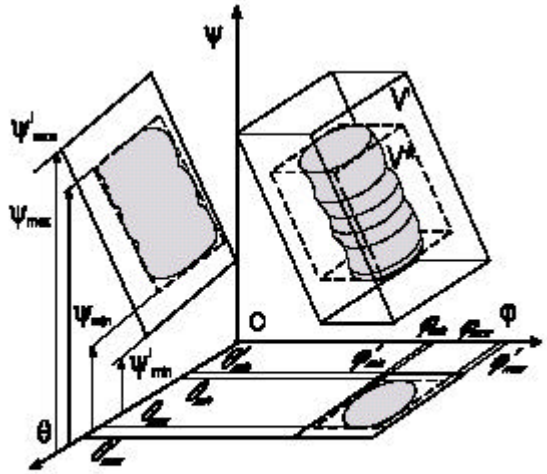

Fig. 2. A numerical approximation for the orientation workspace volume of CaPaMan manipulator.

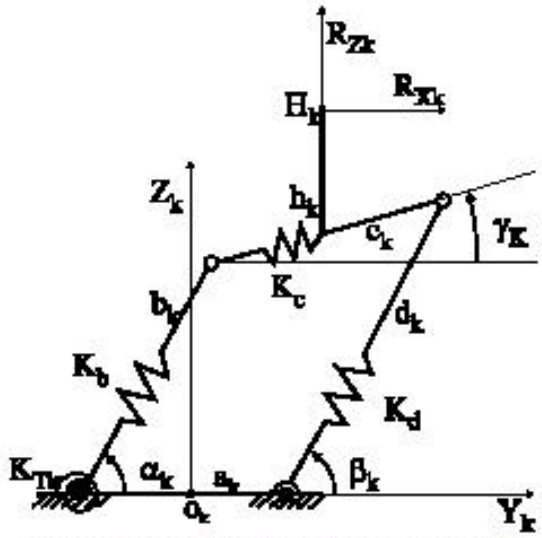

Fig.6 A scheme for stiffness evaluation of a CaPaMan leg.

$$K_{CaPaMan} = M_{FN}\, K_P\, C_P^{-1}\, A_d^{-1}$$

$$G = (9\, r_P^2) / (\, 2b_k^2)$$

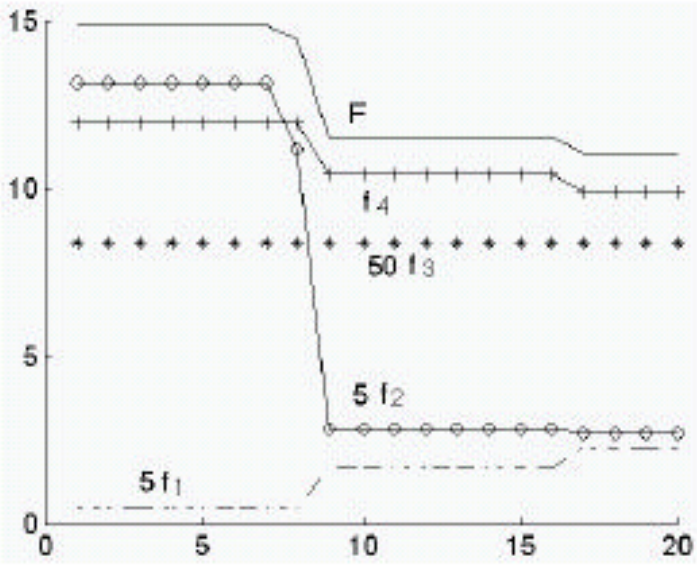

Fig. 7. Evolution of the function F of Eq. (1) and components of Eq. (15) versus number of iterations: position workspace volume as f_1; orientation workspace volume as f_2; compliance displacements and rotations as f_3; singularity condition as f_4.

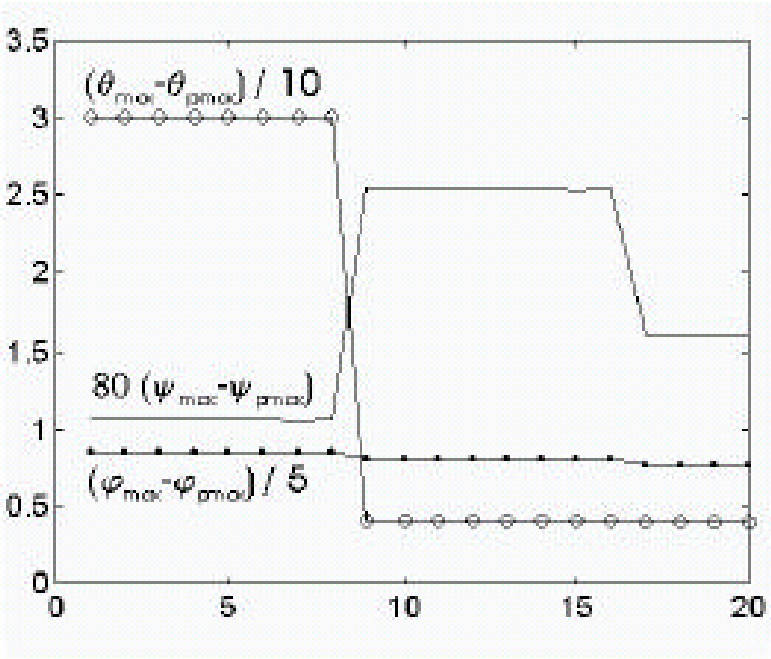

Fig. 8. Evolution of constraints of Eqs. (16) and (17) versus number of iterations for the case of Table 1. (angles are expressed in deg).

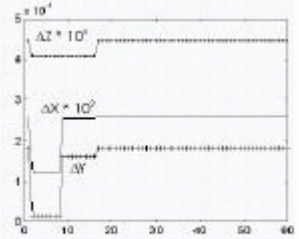

Fig. 9. Evolution of compliance displacements versus number of iterations for the case of Table 1. ΔX, ΔY, and ΔZ; (lengths are expressed in mm).

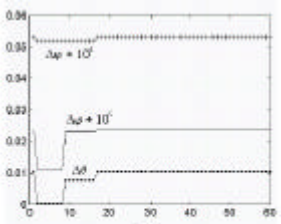

b)

Fig. 10. Evolution of compliance displacements versus number of iterations for the case of Table 1. Δφ, Δψ, and Δθ. (angles are expressed in deg).

5. A CASE OF STUDY: A MACRO-MILLI SERIAL-PARALLEL ROBOTIC MANIPULATOR

In this work we report an application that has been investigated by using hybrid system composed by a serial robot and a parallel manipulator.

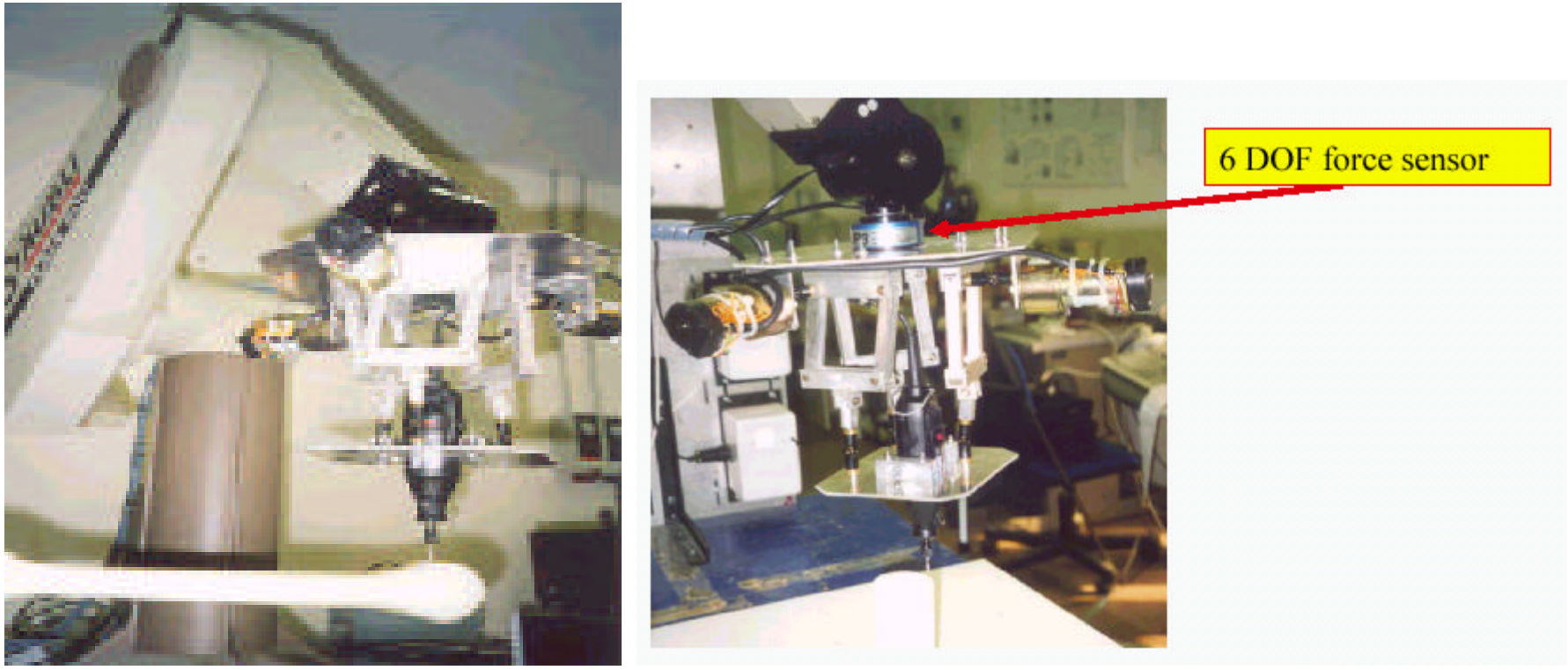

a) b)

Figure 18. A serial-parallel macro-milli manipulator composed of an industrial robot Puma 652 and CaPaMan2 prototype at LARM in Cassino: a) the overall system; b) the wrist parallel manipulator CaPaMan2.

VIDEO

Experimental Results

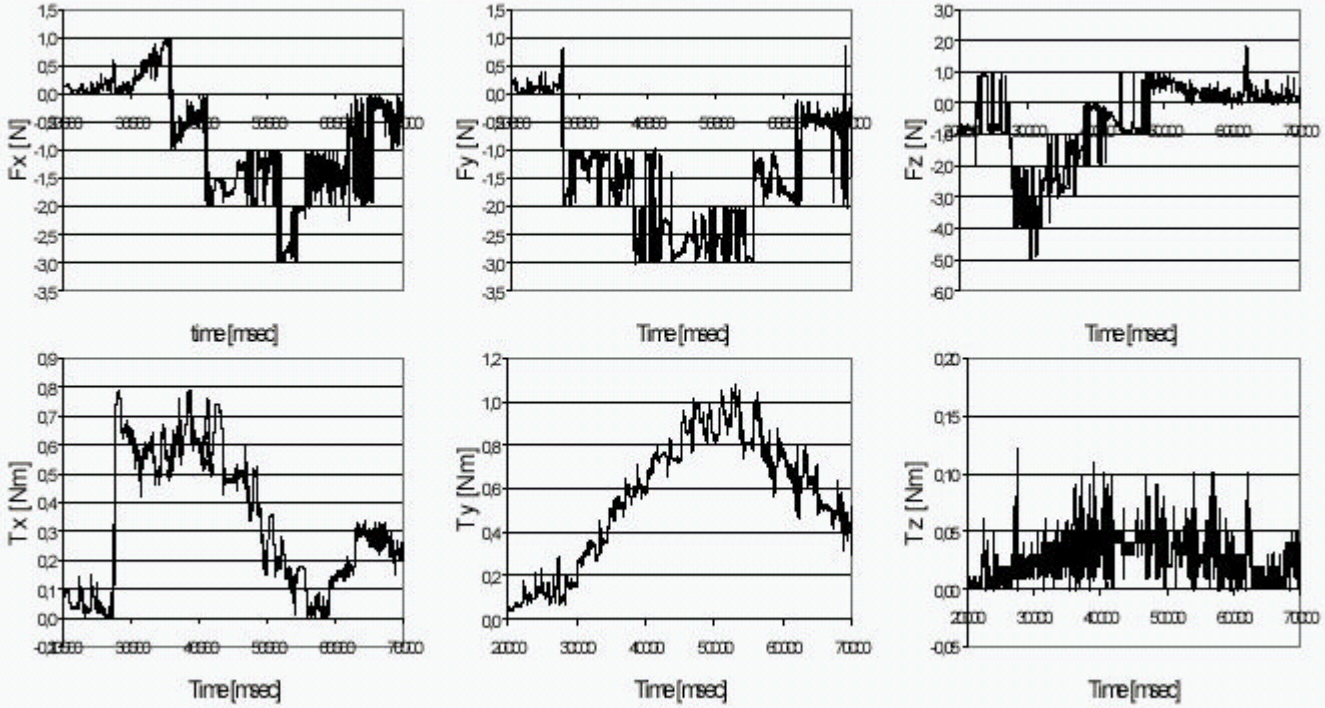

Forces and torques measured on the macro-milli serial-parallel robotic manipulator

Experimental Results

- Maximum force: 8N
- Maximum Torque: 1NM
- Accuracy*:
  expected diameter: 3mm, measured: 3.1mm.
  expected depth of hole: 5mm, measured: 5.2mm.

6. CONCLUSION

In this overview

we have presented parallel manipulators as suitable for assembling operations

with better performances than those of serial chain manipulators.

Character	***Serial Robot***	***Parallel Manipulator***
Links	Open Chain	Close Chain
Workspace	Large	Small
Singularity	Lost DOF	Gain uncontrollable DOF
Structure Stiffness	Low	High
Load/weight ratio	Small	High
Accuracy	Low	Very high
Time respond	Low	High

- significance of an optimum design formulation for parallel manipulators.
- A multi-objective optimization problem
  is formulated as synthetic view of the presented survey but a rational basis for designing parallel manipulators.